JOC The Journal of Organic Chemistry

US University of Sussex

Subscriber access provided by University of Sussex Library

Article

Design, Synthesis, and Characterization of Binaphthalene Precursors as Photo-Activated DNA Interstrand Cross-Linkers

Zechao Lin, Heli Fan, Qi Zhang, and Xiaohua Peng

J. Org. Chem., **Just Accepted Manuscript** • DOI: 10.1021/acs.joc.8b00642 • Publication Date (Web): 22 Jun 2018

ACS Publications

is published by the American Chemical Society. 1155 Sixteenth Street N.W., Washington, DC 20036

Design, Synthesis, and Characterization of Binaphthalene Precursors as Photo-Activated DNA Interstrand Cross-Linkers

Zechao Lin, Heli Fan, Qi Zhang, and Xiaohua Peng*

Department of Chemistry and Biochemistry and the Milwaukee Institute for Drug Discovery, University of Wisconsin-Milwaukee, 3210 N. Cramer Street, Milwaukee, Wisconsin, 53211, United States

pengx@uwm.edu

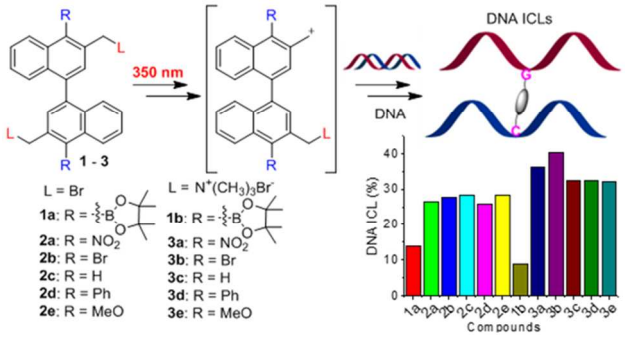

Supporting Information Placeholder

ABSTRACT: Most recently, alkylation via photo-generated carbocations has been identified as a novel mechanism for photo-induced DNA interstrand cross-link (ICL) formation by bifunctional aryl compounds. However, most compounds showed a low efficiency for DNA cross-linking. Here, we have developed a series of new 1,1'-binaphthalene analogues that efficiently form DNA ICLs upon 350 nm irradiation via generated 2-naphthalenylmethyl cations. The DNA cross-linking efficiency depends on the substituents at the position-4 of the naphthalene moiety as well as the leaving groups. Compounds with NO_2, Ph, H, Br, or OMe substituents led to 2-4 times higher DNA ICL yields than those with a boronate ester group. Compounds having trimethyl ammonium salt as a leaving group showed slightly better cross-linking efficiency than those with bromo as a leaving group. Some of these compounds showed a better cross-linking efficiency than that of traditional alkylating agents, such as nitrogen

mustard analogues or quinone methide precursors. These highly efficient photo-activated carbocation precursors allow determination and characterization of the adducts formed between the photo-generated naphthalenyl cations and four natural nucleosides, indicating that the alkylation sites for these naphthalene analogues are dG, dA, and dC.

INTRODCUTION

Photochemical DNA cross-linking agents have attracted attention for a variety of biological applications.[1, 2] They are used as antitumor and anticancer agents[3, 4], for studying DNA damage and repair[5], for photo-manipulation of DNA and therapeutic gene modulation[6], and for constructing DNA photo-switches[7, 8]. Over the past few decades, several research groups have been focused on studies involving photo-induced DNA cross-linking, leading to the discovery of a wide variety of photochemically activated DNA alkylating agents.[1, 2] Several reactive intermediates are involved in photo-induced DNA cross-linking processes, such as quinone methides (QMs), free radicals, and carbocations.[1] Both nucleoside analogues and bifunctional aryl compounds have been developed to generate DNA ICL formation upon photo-induction. For example, the research groups of Zhou[9, 10]and Freccero[11-13] discovered a series of bifunctional phenol, biphenol or binol derivatives that are activated by photo-irradiation to produce QMs directly cross-linking DNA. However, fairly limited examples have been reported to produce DNA ICL products via photo-generated carbocations. Most recently, Li[14] and Greenberg[15] demonstrated that photoirradiation of the modified thymidines generated 5-(2'-deoxyuridinyl)methyl cations that directly produced DNA ICL products. Then, Peng and coworkers found that several aryl boronates and bisnitroimidazole compounds induced DNA ICL formation via photo-generated carbocations.[16-18] However, most of these compounds showed a low efficiency for DNA cross-linking and/or required high concentrations of the substrates. For example, only 10% DNA ICL yield was observed for bisnitroimidazole compounds,[16] 8% for bisnaphthalene boronates,[18] about 2-14% for most benzene derivatives except for methoxybenzene analogues.[17] Development of new

compounds with efficient DNA cross-linking efficiency are essential for further investigation and biological applications.

The structure of naphthalene consists of a fused pair of benzene rings. They have the potential to be applied in cellulo as they would undergo activation using light in visible region of spectra (wavelength > 350 nm) that is either not or only slightly absorbed by most biological molecules and is compatible with living cells. Freccero and co-workers reported that several 2,2'-hydroxyl 1,1'-binaphthalene analogues undergo UV-vis photoactivation to produce binol-quinone methide capable of bisalkylation and DNA cross-linking.[12] In addition, several Binol-amino acid conjuagtes were found to undergo mild photoactivation to yield alkylating and DNA cross-linking agents with high photo-efficiency and superior cytotoxicity.[19] We have recently shown that binaphthalene boronates (**1a** and **1b**, Scheme 1) could be activated by 350 nm irradiation to generate free radicals that are oxidized to the corresponding carbocations directly producing DNA ICL products.[18] However, the DNA cross-linking efficiency of **1a** and **1b** is low with a maximum DNA ICL yield of 11.1% for **1a** and 7.1% for **1b**.

The primary goals of the study presented herein were to find ways of improving the efficiency for photogeneration of carbocations and subsequent DNA ICL formation via a systematic study on the structure-reactivity relationships using the tools of chemical modifications. To this end, we designed and synthesized a series of novel binaphthalene analogues (**2a-e** and **3a-e)** with various aromatic substituents and leaving groups and tested the influence of chemical structure on the carbocation generation, DNA cross-linking efficiency, cross-linking sites, and the overall mechanism for DNA ICL formation. In addition, we will also compare the DNA ICL efficiency of these new compounds to that of **1a** and **1b** that are precursors of cations and quinone methides. Comparison of **2a-e** and **3a-e** to **1a** and **1b**, conveniently absorbing at similar wavelengths, allows an evaluation of the relative cross-linking potency, reducing the effects due to poor absorption (SI, Figure S1). This study is part of a more comprehensive study aimed at exploiting the promising features of binaphthalene compounds as precursors of bisalkylating carbocations.

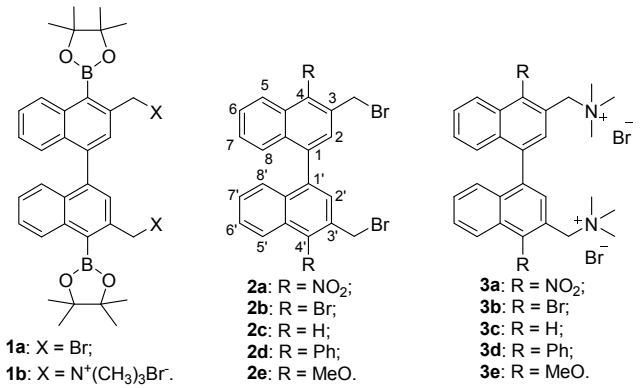

Scheme 1. Bifunctional naphthalene derivatives **1-3**.

RESULTS AND DISCUSSION

Synthesis of bifunctional binaphthalene derivatives. We first synthesized the bromides **2a-e** that were readily converted by nucleophilic substitution to the ammonium salts **3a-e** (Scheme 1). In general, two synthetic routes were employed to synthesize 4,4'-bisubstituted 1,1'-binaphthalene analogues **2a-e**, either via direct coupling reaction of the corresponding 4-substitued mononaphthalene precursor (Scheme 2A and 2B) or via 4,4'-bisbromo-1,1'-binaphthalene analogue **5** by replacing 4-bromo group with the desired substituents (H, NO_2, or phenyl group) (Scheme 2C). Compound **2b** was synthesized via a lead-catalyzed coupling reaction of the 4-bromonaphthalene precursor (**4** → **5**) followed by bromination with *N*-bromosuccinimide (NBS) and azobisisobutyronitrile (AIBN) (Scheme 2A). Similarly, coupling reaction of 4-methoxy naphthalene analogue **7** with $Pb(OCOCH_3)_4$ as a catalyst provided 1,1'-binaphthalene **8** that was converted to **2e** via reduction (→**9**) followed by bromination (→**2e**) (Scheme 2B). An electron-donating group (OMe) favored the lead-catalyzed coupling reaction (42% for **8** vs. 18% for **5**). However, direct coupling reaction of the naphthalenes with H, nitro, or phenyl group at the position-4 failed to yield the desired 1,1'-binaphthalene products. The lead-catalyzed coupling reaction of 2-methylnaphthalene generated 3,3'-dimethyl-1,1'-binaphthalene (**10**) and several by-products with similar polarity, which hindered purification by column chromatography. Direct coupling reaction of commercially available 2-methyl-1-nitronaphthalene did not occur possibly

due to the strong electron withdrawing effect of the nitro group prohibiting the reaction. Thus, **2a**, **2c**, and **2d** were synthesized starting from a more general precursor **5**. Debromination of **5** was carried out with n-BuLi yielding **10** that was converted to **2c** by treatment with NBS/AIBN. Nitration of **10** using HNO_3/AcOH generated 4,4'-dinitro-1,1'-binaphthalene **11** that was brominated using NBS/AIBN yielding **2a**. A phenyl group was introduced by palladium-catalyzed coupling reaction of **5** yielding 3,3'-dimethyl-4,4'-diphenyl-1,1'-binaphthalene (**12**). Bromination of **12** using NBS/AIBN produced **2d**. Finally, **2a-e** were converted to the corresponding ammonia salts **3a-e** by treatment with trimethyl amine in ethyl acetate in almost quantitative yields.

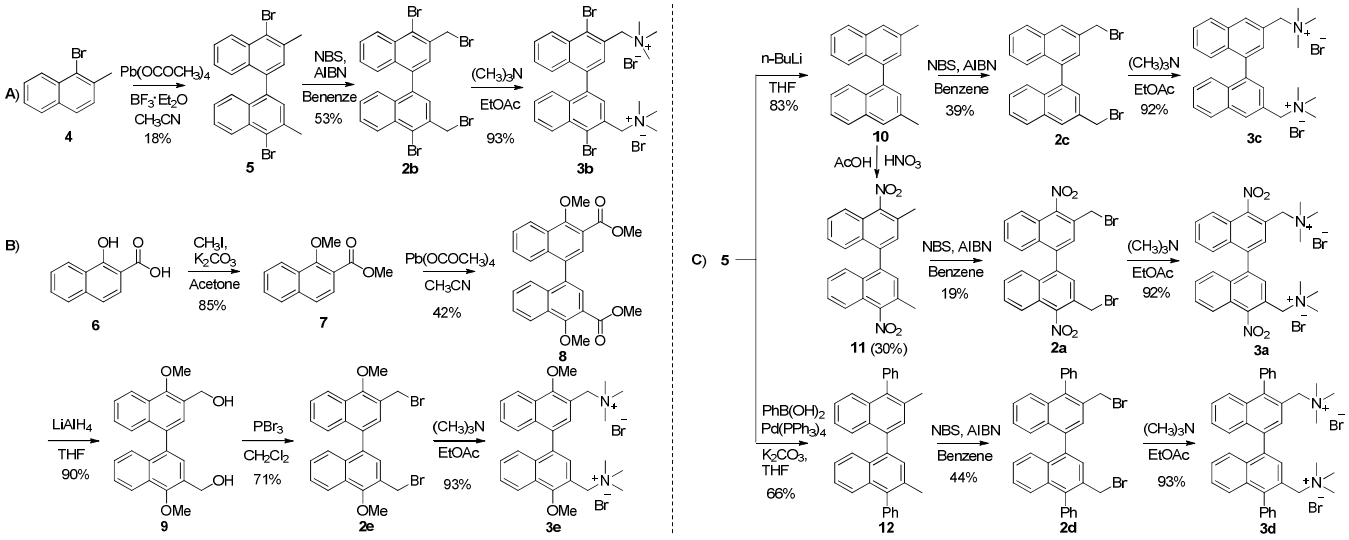

Scheme 2. Synthesis of bifunctional binaphthalene derivatives **2a-e** and **3a-e**.

DNA interstrand cross-linking assay. With the availability of 4,4'-disubstituted 1,1'-binaphthalene analogues **2a-e** and **3a-e**, we investigated the substituent effects on the photo reactivity of these compounds towards DNA by measuring DNA ICL formation upon irradiation with 350 nm light. Similar to our previous study[18], a 49-mer DNA duplex **13** was used for this study. Initially, 500 μM of the substrates were used and the reaction mixture was irradiated by 350 nm light for 6 h. DNA ICL formation and cross-linking yields were analyzed via denaturing polyacrylamide gel electrophoresis (PAGE) with phosphorimager analysis (Image Quant 5.2). As these compounds showed different water

solubility that could in turn affect their DNA cross-linking efficiency, we optimized the reaction conditions for DNA interstrand cross-linking assay in order to find a condition suitable for all substrates. First, we explored the effect of solvents on DNA ICL formation induced by these compounds. As some of these compounds are lipophilic and showed poor water solubility, a miscible organic solvent, such as MeCN, MeOH, DMF, THF, and DMSO, was added as an auxiliary solvent to improve the solubility. As a representative, the result for **3b** is illustrated in the supporting information (SI, Figure S2). Compared with the pure water reaction system, the addition of organic solvents improved the cross-linking efficiency (SI, Figure S2, line 2 vs line 3-7). A mixture of water and acetonitrile (7:3) showed the highest promoting effect, leading to 11% increase of DNA ICL yield of **3b** (SI, Figure S2, lane 3, 30.3% yield). Second, the effect of the pH values on DNA cross-linking was investigated using a phosphate buffer system (SI, Figure S3). The DNA cross-linking yields of 37% – 39% were observed with a pH value ranging from 6.0 to 8.0, while a phosphate buffer with a pH higher than 8.7 or lower than 5.0 led to decreased DNA ICL yields (30.9% at pH 5 and 34.5% pH 8.7). In addition, compared to pure H_2O system (19.8%), a phosphate buffer of pH 6 - 8 greatly increased the DNA cross-linking efficiency. However, DNA damage was observed under strong basic or acidic conditions (pH 12.6 and pH 4.5) (SI, Figure S3, lanes 2 and 8). Finally, a mixture of pH 8 phosphate buffer and acetonitrile (7:3) was used for further investigation.

Our previous study showed that the DNA cross-linking efficiency depended on the irradiation time and the concentration of the substrate.[18] For better comparison of the reactivity of these naphthalene analogues towards DNA and the effect of the aromatic substituent and the leaving group on DNA ICL formation, we determined the optimal reaction time for DNA cross-linking induced by **2a-e** and **3a-e** and the compound concentration required to saturate alkylation sites in DNA. Study on time-dependent DNA ICL formation showed that the DNA cross-linking reaction is complete within 8-11 h for these compounds (Table 1 and SI, Figures S4-13). DNA damage was observed when the irradiation time was longer than 24 h. The aromatic substituents and leaving groups only slightly affect the reaction rate of

these naphthalene analogues. With the optimized reaction time, we determined the minimum concentrations required to obtain the best DNA cross-linking efficiency for **2a-e** and **3a-e**. Generally, the cross-linking efficiency was gradually improved with an increase in the concentration of the compounds. The DNA cross-linking reaction reached a balance for **2a-e** at 0.5 mM concentration, while a little higher concentration (about 1.0 mM) was required for **3a-e** to saturate the alkylation sites (SI, Figure S14-23).

With the optimized conditions for all compounds, we were able to compare their DNA cross-linking efficiency. As these compounds absorb at similar wavelengths reducing the effects due to poor absorption (SI, Figure S1), comparison of **2a-e** and **3a-e** to the existing binaphthalene boronate esters **1a** and **1b** allows an evaluation of the relative cross-linking potency. In comparison with **1a** and **1b**, all new compounds greatly improved the DNA ICL yields. For example, the ammonium salts **3a-e** led to 2-4 times higher ICL yields than **1b** (Figure 1, Table 1). Similarly, the bromides **2a-e** showed 12%-15% higher ICL yields than **1a**. We speculated that **1a** and **1b** may be more difficult to insert into the DNA duplex structure due to the steric-hindrance of the boronate ester group. The ICL efficiency of these photo-activated alkylating agents (**2a-e** and **3a-e**) are comparable to or better than traditional DNA cross-linking agents such as nitrogen mustard analogues (e.g. 20%-44% for 4-[bis(2-chloroethyl)amino]phenol analogues at 1.0 mM concentration)[20, 21] or quinone methide[22] precursors. Among **2a-e** and **3a-e**, compounds with a trimethyl amine as a leaving group showed slightly higher DNA cross-link yields than those with Br as a leaving group. Compound **3b** with a 4-bromo substituent provided the highest DNA cross-linking efficiency (Table 1). However, the introduction of NO_2, Ph, or OMe on the parent compound **2c** or **3c** did not show obvious effects for photo-induced DNA ICL formation of the binaphthalene moieties.

Table 1. The optimized conditions and ICL yields for **1-3**.[a]

Bromides	Rea. Time (h)	ICL yields (%)[c]		Ammonia Salts	Rea. Time (h)	ICL yields (%)[c]	
		0.5 mM[b]	1.0 mM			0.5 mM	1.0 mM[b]

1a (R = Boronate)	8	13.8 ± 0.7	13.8 ± 0.9	**1b** (R = Boronate)	4	8.7 ± 1.0	8.7 ± 0.8
2a (R = NO_2)	8	25.6 ± 1.5	26.4 ± 1.0	**3a** (R = NO_2)	10	33.2 ± 1.5	36.2 ± 1.6
2b (R = Br)	8	28.3 ± 1.2	27.8 ± 1.2	**3b** (R = Br)	10	36.3 ± 1.8	40.2 ± 1.7
2c (R = H)	10	28.1 ± 2.1	28.4 ± 2.0	**3c** (R = H)	11	30.6 ± 1.5	32.6 ± 1.5
2d (R = Ph)	10	25.6 ± 1.1	25.8 ± 1.3	**3d** (R = Ph)	11	29.3 ± 1.2	32.5 ± 1.3
2e (R = OMe)	10	28.6 ± 1.0	28.4 ± 1.6	**3e** (R = OMe)	10	30.8 ± 1.1	32.0 ± 1.0

[a] The DNA cross-linking reaction was performed in a mixture of pH 8 phosphate buffer and MeCN (7:3) with 50 nM DNA duplex **13** upon 350 nm irradiation.
[b]The minimum compound concentration needed to obtain the best cross-linking efficiency.
[c] The maximum DNA ICL yield obtained for each compound under optimized conditions (all data are the average of three experiments).

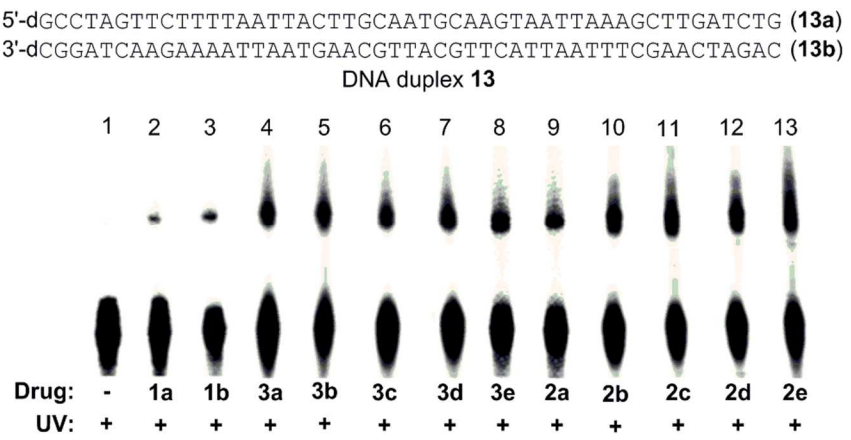

Figure 1. UV-induced DNA cross-link formation by **1a**, **1b**, **2a**-**e**, and **3a**-**e**. Lane 1: DNA only; lane 2: 0.5 mM **1a** (13.8%, 8 h); lane 3: 0.5 mM **1b** (8.7%, 4 h); lane 4: 1 mM **3a** (34.8%, 10 h); lane 5: 1 mM **3b** (39.2%, 10 h); lane 6: 1 mM **3c** (32.6%, 10 h); lane 7: 1 mM **3d** (32.5%, 10 h); lane 8: 1 mM **3e** (32.0%, 10 h); lane 9: 0.5 mM **2a** (25.6%, 8 h); lane 10: 0.5 mM **2b** (27.1%, 8 h); lane 11: 0.5 mM **2c** (28.1%, 10 h); lane 12: 0.5 mM **2d** (28.8%, 10 h); lane 13: 0.5 mM **2e** (31.6%, 10 h) [Irradiated at pH 8 phosphate buffer and mixture solvent of MeCN/H_2O (3:7). ODN **13a** was labelled with ^{32}P at the 5'-termini].

Mechanism of DNA ICL formation. In our previous work, we have revealed that photo-induced DNA ICL formation of several arylboronates was via carbocation formation[17, 18]. The pathway for generating the carbocation intermediate **A** strongly depends on the substrates (Scheme 3a). The benzyl cations were generated either via direct heterolysis of a C-X bond (Pathway 1) or oxidation of a free radical **B** (Pathway 2), which was dependent on the leaving groups.[17] For binaphthelene boronates **1a** and **1b**, the carbocations that directly cross-link DNA were generated via oxidation of the corresponding free radical

B (Scheme 3a, Pathway 2).[18] However, only two compounds have been reported so far for the category of naphthalene compounds and both contain a boronate group, which is not sufficient to fully understand the property of this novel mechanism. In order to test the generality of this mechanism, we investigated the DNA cross-linking mechanism of **2a-e** and **3a-e** by determining the reactive intermediates responsible for DNA ICL formation. Two orthogonal traps, methoxyamine and 2,2,6,6-tetramethylpiperidin-1-oxyl (TEMPO) that can trap carbocations and free radicals respectively, were employed for this study. The two traps were then tested separately as competitors for DNA ICL formation upon 350 nm irradiation of **2a-e** and **3a-e** with DNA duplex **13**. The effect of methoxyamine and TEMPO on DNA ICL formation induced by **2b** and **3b** is illustrated in Figure 2, while the data of all other compounds are presented in Figures S24-43. The addition of either methoxyamine or TEMPO decreased DNA cross-linking yields of **2b** and **3b**, suggesting that both methoxyamine and TEMPO inhibited DNA ICL formation induced by **2b** and **3b** (Figure 2). The cross-link yield of **3b** decreased from 31.4 ± 1.5% to 1.8 ± 0.7% with 100 mM methoxyamine and from 32.8 ± 1.3% to 2.4 ± 0.6% with 100 mM TEMPO (Figure 2B). Complete quenching of DNA ICL formation by methoxyamine indicated that the carbocation intermediates directly cross-linked DNA, while complete inhibition of DNA ICL formation by the radical trap suggested that the cation intermediates were generated via oxidation of the corresponding free radical (pathway 2) not by direct heterolysis of a C-X bond (pathway 1). This is consistent with our previous study for **1a** and **1b**.[18] Based on these observations, we proposed that 350 nm irradiation of **2b** or **3b** generated the 2-naphthalenylmethyl free radical **14b** that was oxidized to the corresponding cation **15b** directly alkylating DNA. Similarly, complete inhibition of DNA ICL formation by methoxyamine and TEMPO was observed with **2a**, **2c-e**, **3a**, and **3c-e** (SI, Figure S24-44), which suggested the generality of this novel mechanism for the naphthalene moieties (Scheme 3).

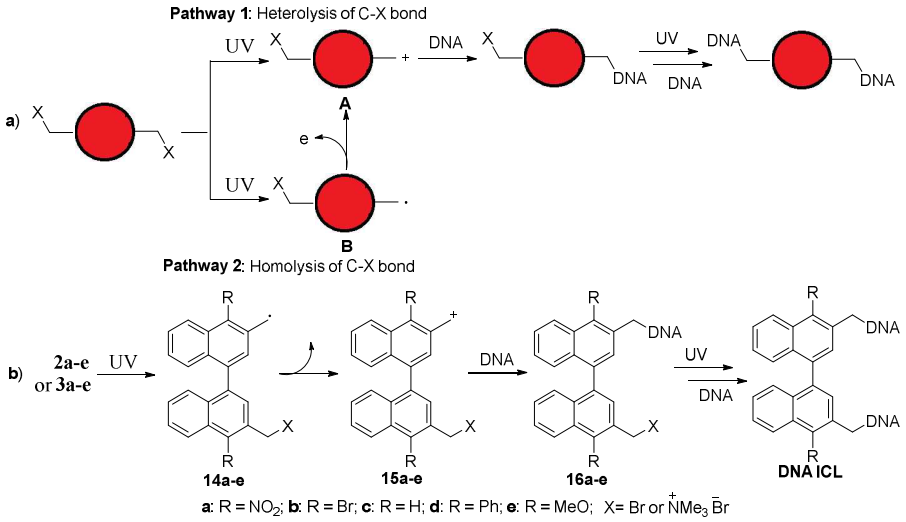

Scheme 3. (A) General mechanisms for photo-induced DNA ICL formation by bifunctional aromatic compounds (represents the aromatic rings); (B) Proposed mechanism for DNA ICL formation induced by **2a-e** and **3a-e**.

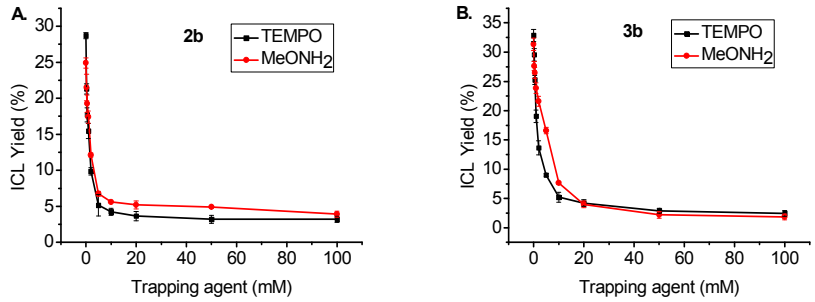

Figure 2. Effect of TEMPO and methoxyamine on ICL formation induced by **2b** (A) and **3b** (B) (DNA duplex **13** was irradiated with 350 nm light in the presence of 0.5 mM **2b** or **3b** at pH 8 for 8 h).

Having demonstrated that both free radicals and carbocations were actively involved in DNA cross-linking process of **2a-e** and **3a-e**, we obtained the carbocation and free radical trapping products using the monomer reactions. The carbocation and free radical trapping reactions were performed with the monomers upon 350 nm irradiation in the presence of excess methoxyamine and TEMPO, respectively. Compounds **2b** and **3b** were chosen as two representatives for this study. The reaction was carried out in

a pH 8.0 phosphate buffer at 37 ºC. As expected, 350 nm irradiation of **2b** or **3b** in the presence of TEMPO provided free radical trapping product **18** while the cation trapping product **21** was obtained in the presence of methoxyamine (Scheme 4). Compound **18** was characterized by NMR and HRMS, while **21** was unstable under the conditions for NMR measurement. Thus, mass spectrometry was used to determine the product. Detection of fragment ion of m/z 528.0040 [IT–TOF–MS (ESI)] suggested formation of **21** (Scheme 4B). In addition, we synthesized a simpler analogue **22** and obtained its cation trapping product **23** by 350 nm irradiation of **22** in the presence of excess methoxyamine (Scheme 4C). This study provided direct evidence for that both free radicals and carbocations were involved in the DNA cross-linking process induced by **2b** and **3b** upon 350 nm irradiation. Collectively, our data provide further evidence for the mechanism proposed for photo-induced DNA ICL formation by these compounds (Scheme 3b).

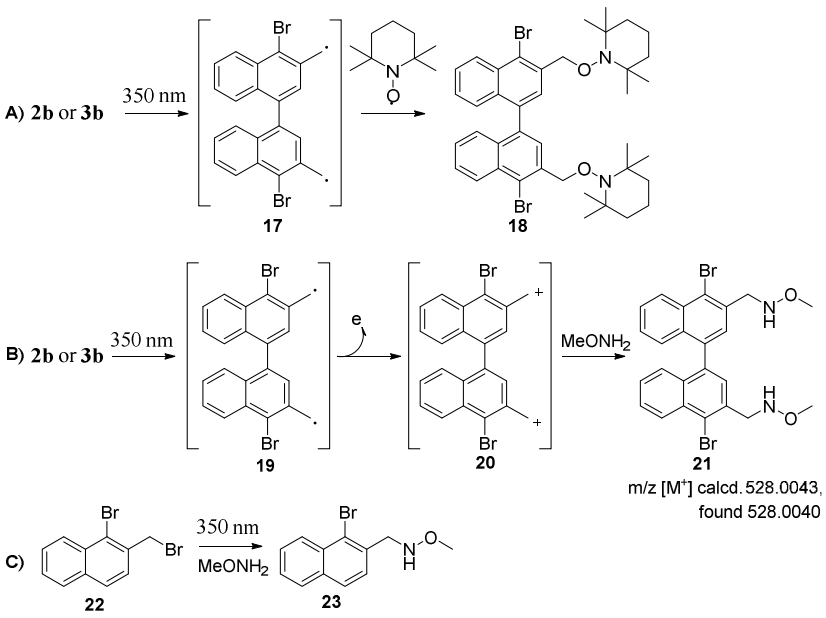

Scheme 4. **A**) Free radical trapping reactions of **2b** and **3b** with TEMPO; **B**) Cation trapping reactions of **2b** and **3b** with methoxyamine; **C**) Cation trapping reaction of **22** with methoxyamine.

Determination of DNA alkylation sites and alkylating products. Testing the stability of the DNA ICL products upon heating under basic or neutral conditions can be used for initial detection of heat-labile and/or alkaline-labile DNA alkylation sites.[21] According to the Maxam and Gilbert reaction mechanism,

it is well known that N7-alkylated purines can be cleaved upon heating in piperidine treatment.[23, 24] Thus, the alkylation sites of **2a-e** and **3a-e** towards DNA were investigated by determining the heat stability of DNA ICL products formed with these compounds. Initially, the stability test of ICL products was performed with crude materials purified by simple precipitation without gel purification. The heat stability data for DNA ICL products formed with **2a-e** are shown in Figures S45. In all cases, the DNA ICL products were destroyed by heating in 1.0 M piperidine for 30 min, while they were more stable to heating in a pH 7 phosphate buffer. DNA cleavage bands were observed mainly at dG sites but only minorly at dA sites upon heating in 1.0 M piperidine (Figure S45, lanes 3, 7, and 11), which indicated that photo-induced DNA alkylation by these compounds mainly occurred with dG. To figure out whether DNA cleavage by piperidine treatment occurred to cross-linked DNA or mono-alkylated DNA or both, we isolated the DNA ICL products formed with **3b** from other alkylated single-stranded DNA species (ODN **13a**') by denaturing PAGE. Similar to the above observation, isolated cross-linked DNA showed higher stability upon heating in pH 7 buffer (Figure 3, lane 5) than in 1.0 M piperidine (Figure 3, lane 6). Similar cleavage patterns (with major cleavages at dG sites) were observed for cross-linked ODN and single-stranded ODN **13a**' upon heating in 1.0 M piperidine (Figure 3, lane 3 vs lane 6). These data suggested that in addition to interstrand cross-linking, intrastrand cross-linking and mono-alkylation could also occur at dG sites.

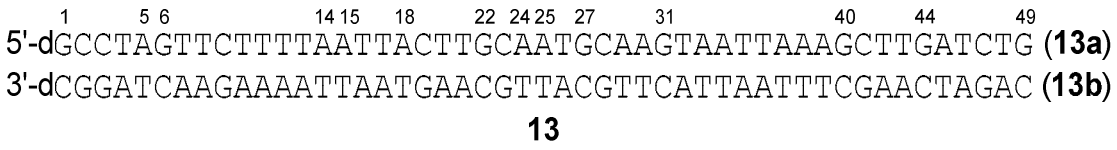

13

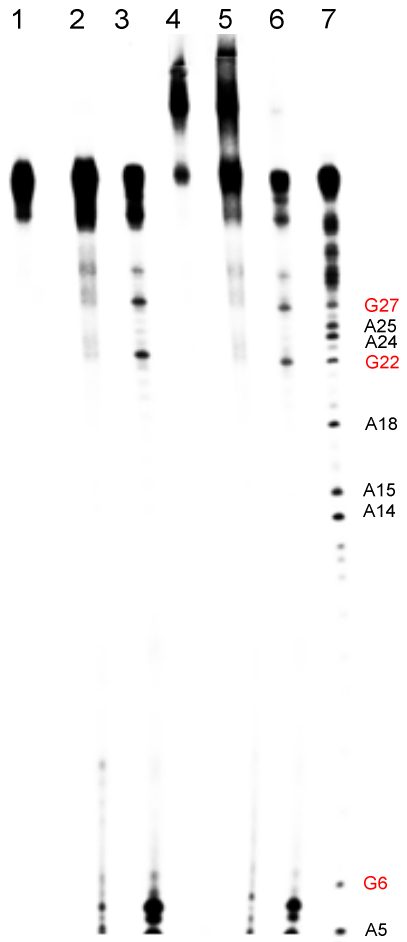

Figure 3. Determination of cross-linking site of **3b**. Phosphorimage autoradiogram of 20% denaturing PAGE analysis of the isolated ICL products and alkylated single-stranded ODN **13a**' upon heating in pH 7 phosphate buffer or piperidine. Lane 1: isolated alkylated single stranded ODN (**13a**'). Lane 2: **13a**' was heated in a pH 7 phosphate buffer at 90 °C for 30 min. Lane 3: **13a**' was heated in 1.0 M piperidine at 90 °C for 30 min. Lane 4: Isolated DNA ICL products. Lane 5: the DNA ICL products were heated in a pH 7 phosphate buffer at 90 °C for 30 min. Lane 6: the DNA ICL products were heated in 1.0 M piperidine at 90 °C for 30 min. Lane 7: G+A sequencing.

Although the heat-stability study of the DNA ICL products provided evidences that the major alkylating sites are dGs, the reaction sites stable to heating could not be detected. Hopkins and co-authors reported that hydroxyl radical cleavage of gel-purified cross-linked DNA could be used to determine the cross-linking site(s) in instances in which multiple alkylation/cross-linking sites are present in a single molecule[25]. Only fragmentation between the radiolabel and the cross-linked nucleotide affords

fragments shorter than starting single strand, and thus the abundance of fragment sizes longer than cross-link sites would decrease, which reveals sites of cross-linking. Instead of the original 49mer DNA duplex **13**, a shorter DNA duplex **27** was used for this study to ensure determination at single nucleotide resolution of DNA fragments by denaturing PAGE. Each oligonucleotide was either 5'-^{32}P- or 3'-^{32}P-labeled. As anticipated, the abundance of dG- or dC- cleavage fragments is higher than that of dA- or dT cleavage fragments. For example, the cleavage pattern of the isolated cross-linked material with 5'-[^{32}P]-labelled **27b** showed that relative to the native sample, the yield of fragments 7 or 8 nucleotides long was diminished relative to fragments 5 or 6 nucleotides long (Figure 4A,B). Similarly, the abundance of cleavage fragments from C46 to T51, C53 to T56, then C58 greatly decreased in comparison with that of G45, G52, or G57 cleavage fragments. These data suggested that the majority of the cross-links occurred with dG. In addition, the ratios of corresponding peak areas from one-dimensional scan of the cross-linked and native samples were calculated (Figure 4C). It was obvious that fragment yields dropped following C42, C46, C49, and C53, indicating that dCs are possible cross-linking sites. Similarly, cleavage pattern of the isolated cross-linked material with 3'-[^{32}P]-labelled **27a** indicated that the cross-links in the complementary strand involved reaction with G31, C28, G27, G24, C21, and G20 (Supporting Information Figure S46). Cleavage pattern of DNA cross-linked products with 5'-[^{32}P]-labelled-**27a** or 3'-[^{32}P]-labeled-**27b** also indicated that the possible cross-link sites are dGs and dCs. However, we could not succeed in any of our efforts in quantification of various interstrand cross-link locations, possibly due to complications of multiple cross-link sites (more than 16 in duplex **27**) and multiple cross-linking events occurred per duplex.

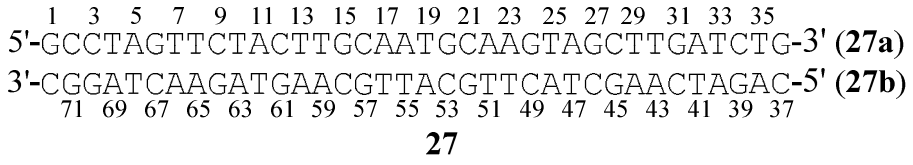

27

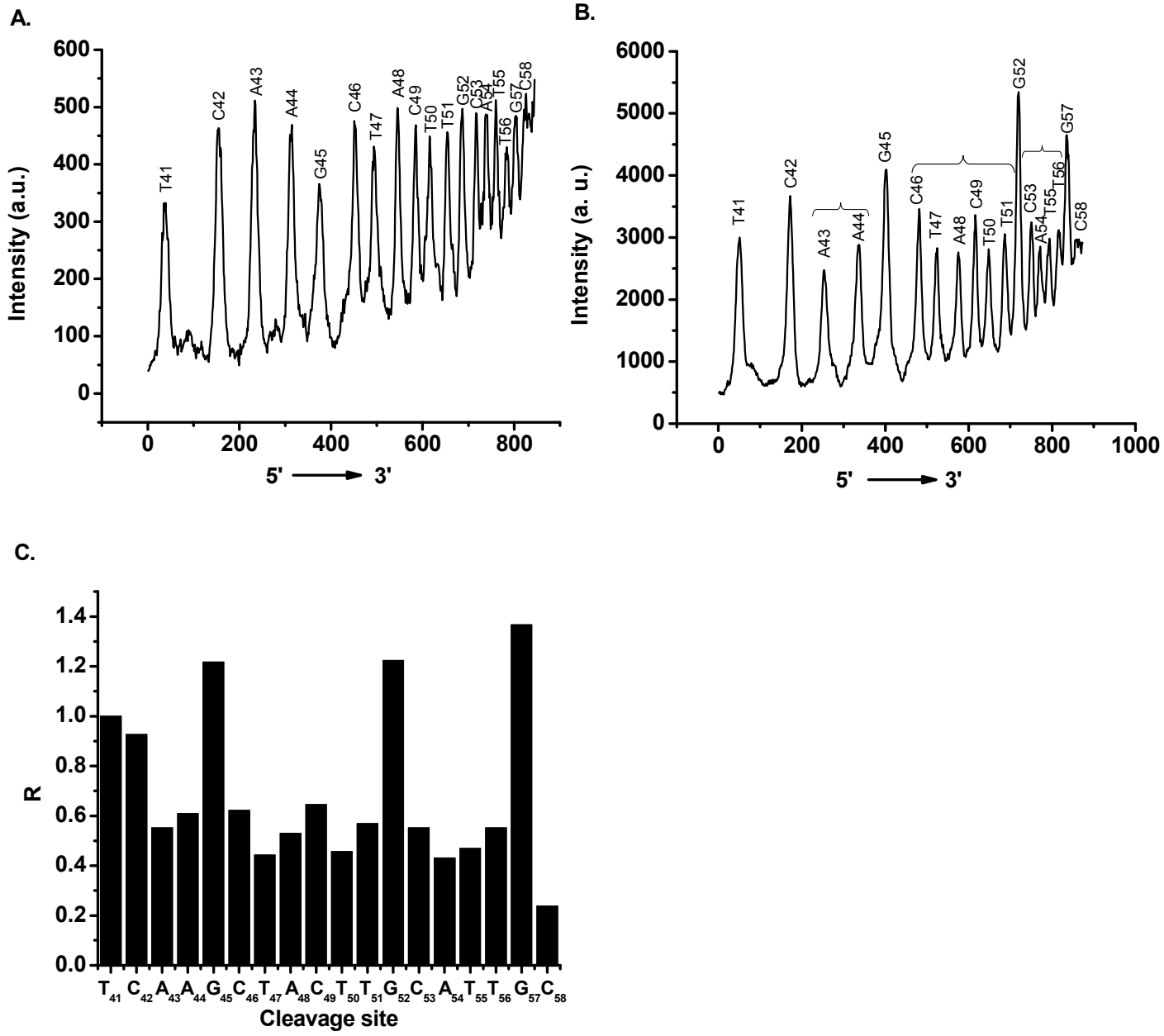

Figure 4. Determination of interstrand cross-linking position via OH· cleavage of **3b**-cross-linked DNA duplex **27**: A) partial fragmentation patterns for native duplex **27** using iron(II)/EDTA; B) partial fragmentation patterns for **3b**-cross-linked **27** using iron(II)/EDTA; C) Ratio of fragment abundance in **3b**-cross-linked and native DNA duplex **27** as a function of cleavage site. ODN **27b** was [^{32}P]-labelled at the 5'-termini.

Previously, the structure of the cross-linked adducts formed by a naphathalene cation have not been determined due to the poor photoreactivity of **1a** and **1b** towards DNA[18]. In order to gather further

evidence for the DNA cross-linking sites of the naphathalene analogues, we performed a monomer reaction by examining the reactivity of photo-generated 2-naphthelenemethyl cation with four canonical nucleosides (dT, dC, dA, and dG). As a representative, **2b** was chosen for this study. Compound **2b** was irradiated in DMF in the presence of dT, dC, dA, or dG with 350 nm light until disappearance of all starting material. Initially, thin layer chromatography (TLC) was used to monitor the reaction, which indicated formation of the new products for dC, dA, and dG but not for dT. The crude products generated between **2b** and dC or dA were further purified by column chromatography providing **24** (41% yield) and **25a** (49% yield), respectively, which were characterized by NMR and HRMS (Scheme 5A and 5B). However, **25a** was unstable and deglycosylation occurred, resulting in **25b** shown by HRMS (Scheme 5B). However, the adducts formed between **2b** and dG were too complex to be purified. In addition, TLC showed that decomposition occurred during the purification process leading to the new by-products. NMR data were not obtained for any **2b**-dG adducts. Finally, HRMS was used to detect adducts formed between **2b** and dG, indicating formation of **26a-d** (Scheme 5C). Deglycosylation of **26b** generated **26d**. Although the molecular ion peak of **26e** was not detected, its deglycosylated product **26c** was observed. Thus, we conclude that the DNA ICL formation induced by these 2-naphthelenemethyl cations occurred with both dG and dC, while mono-alkylation would also occur with dA, dG, and dC.

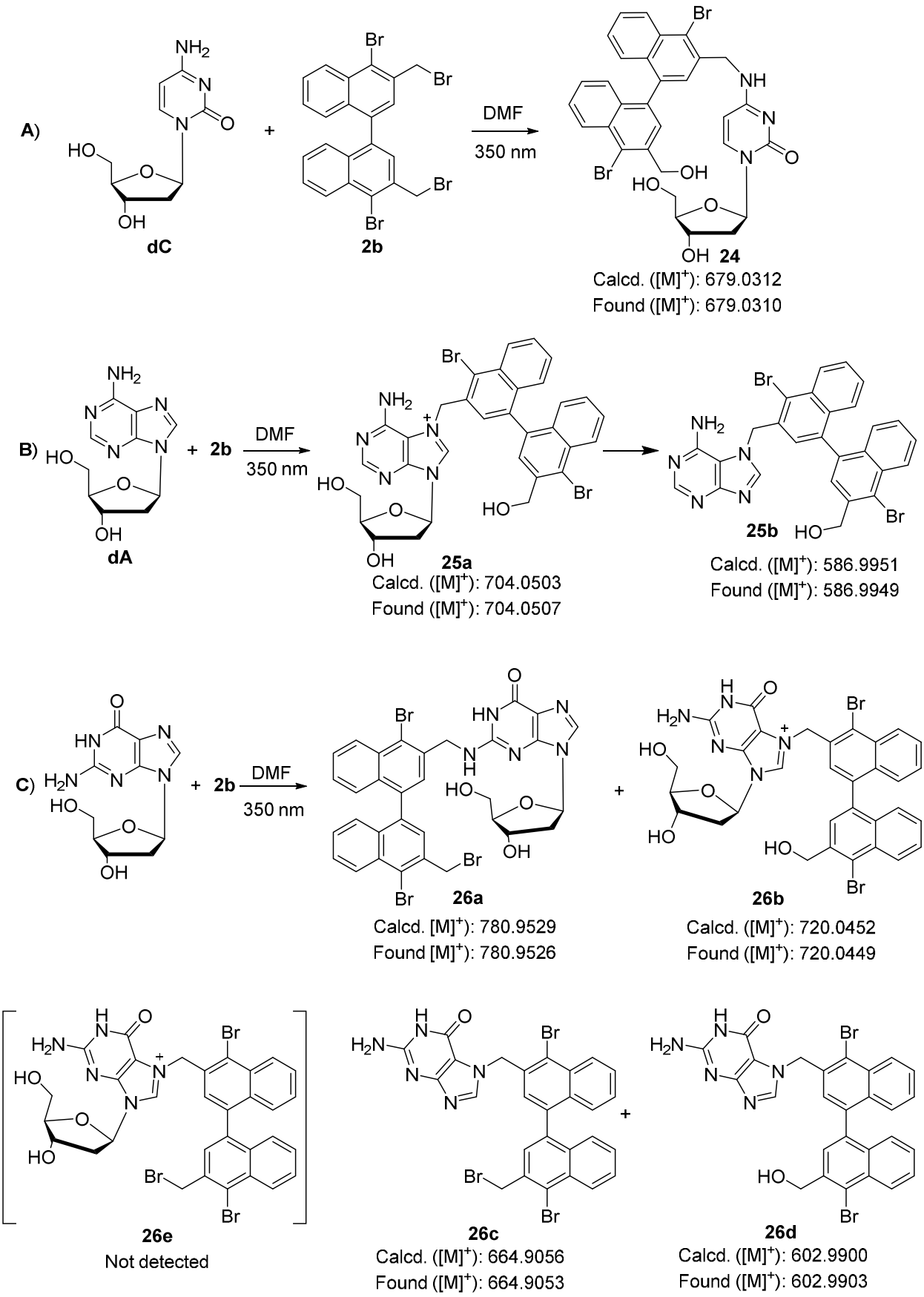

Scheme 5. Monomer reactions of **2b** and the nucleosides dG, dA, and dC.

CONCLUSION

Carbocation formation has been discovered to be an important mechanism for photo-induced DNA cross-linking by bifunctional aryl compounds,[17, 18] such as 1,1'-binaphthalene boronate esters **1a** and **1b**. However, very low ICL efficiency was observed with **1a** and **1b**. Here, we performed a structure-reactivity relationship study and discovered a series of bifunctional naphthalene compounds as highly efficient photo-induced DNA cross-linking agents. The aromatic substituents at the position-4 of the naphthalene moiety and the leaving groups affect the DNA cross-linking efficiency. Compounds containing nitro, bromo, hydrogen, phenyl, or methoxy showed 2-4 times higher cross-linking potency than **1a** or **1b** with boronate ester. Trimethyl ammonium salt as a leaving group led to slightly higher DNA cross-linking efficiency than bromo as a leaving group. These compounds showed a DNA cross-linking mechanism similar to **1a** and **1b**. They can be activated by 350 nm irradiation to generate free radicals that are oxidized to the corresponding carbocations directly producing DNA ICL products. The discovery of these highly efficient photo-activated DNA interstrand cross-linkers allowed us to determine the adducts formed between the photo-generated naphthalene cations and four canonical nucleosides. Alkylation reaction of the photo-generated 2-naphthelenemethyl cation occurred with dG, dC, and dA. Development of new compounds with efficient DNA cross-linking efficiency are essential for further investigation and biological applications.

EXPERIMENTAL SECTION

General Information. Unless otherwise specified, all chemicals and reagents were commercially purchased and were used as received without further purification. Thin-layer chromatography (TLC) was carried out on precoated silica gel plates and visualized under UV light. Oligonucleotides were synthesized via standard automated DNA synthesis techniques. Deprotection of the synthesized DNA were performed under mild deprotection conditions using a mixture of 40% aqueous $MeNH_2$ and 28% aqueous NH_3 (1:1) at room temperature for 2 h. Oligonucleotides were purified by 20% denaturing PAGE. [γ-^{32}P] ATP was used for DNA labeling with standard method.[26] Quantification of radiolabeled

oligonucleotides was carried out using a Molecular Dynamics phosphorimager equipped with ImageQuant, version 5.2, software. For all Phosphorimage autoradiogram, the top dark spot that migrated slowest is considered as DNA cross-link product and the bottom dark spot considered as the single-stranded ODN, which were determined using molecular ladder.[20] ^{1}H NMR and ^{13}C NMR spectra were collected on a Bruker DRX 500 MHz or 300 MHz spectrophotometer with TMS as internal stander. High resolution mass spectrometry was performed at the University of Wisconsin-Milwaukee Mass Spectrometry Lab on a Shimadzu LCMS-IT-TOF mass spectrometer equipped with an atmospheric-pressure chemical ionization (APCI) or electron spray injection (ESI).

Compound Synthesis and Characterization.

*4,4'-Dibromo-3,3'-dimethyl-1,1'-binaphthalene (**5**)*. Boron trifluoride diethyl etherate (20 mL) was added to a solution of 1-bromo-2-methylnaphthalene (**4**) (17.68 g, 0.08 mol) and lead tetraacetate (19.52 g, 0.044 mol) in acetonitrile (100 mL). The reaction mixture was stirred overnight, then poured into water (300 mL), and the products were extracted with dichloromethane (2 x 300 mL). The organic layer was dried over Na_2SO_4, filtrated, and evaporated. The crude product was passed through a short column of basic alumina using hexane as eluent to remove the Pb and highly colored polymeric materials, then purified through column chromatography (2.5% EtOAc/Hexane) to provide **5** (3.09 g, 18%) as a white solid. ^{1}H NMR (300 MHz, $CDCl_3$): δ 8.44 (d, J = 4.4 Hz, 2H), 7.59 (t, J = 4.5 Hz, 2H), 7.39 (s, 2H), 7.32-7.28 (m, 4H), 2.71 (s, 6H) (the NMR spectra were in agreement with those reported). [18, 27]

*3,3'-Dimethyl-1,1'-binaphthalene (**10**).* n-BuLi (5.8 mL, 9.2 mmol, 1.6 M in hexane) was added to a solution of **5** (1.0 g, 2.3 mmol) in THF (30 mL) at -78 ℃. The reaction mixture was stirred about 4 h. Then, water (15 mL) was added. After the reaction mixture was stirred overnight, THF was removed under vacuum. The remaining aqueous phase was extracted with dichloromethane (3 x 15 mL). The organic layer was dried over $MgSO_4$, filtrated, and evaporated. The crude product was purified through column chromatography (pure hexane) to provide **10** as a white solid (539 mg, 83%). ^{1}H NMR (300 MHz, $CDCl_3$): δ 7.90 (t, J = 6.1 Hz, 2H), 7.77 (br, 2H), 7.50-7.40 (m, 6H), 7.27 (d, J = 6.3 Hz, 2H), 2.64 and 2.62 (2S, 6H).

*4,4'-Dinitro-3,3'-dimethyl-1,1'-binaphthalene (**11**).* Compound **10** (1.0 g, 3.5 mmol) was dissolved in glacial acetic acid (15 mL), then 70% HNO_3 (5 mL) was added with stirring in an ice bath. The reaction mixture was stirred at r.t. for 24 h. TLC (Hexane/CH_2Cl_2 = 10/1) showed that the reaction was complete with disappearance of **10**. Water (10 mL) was added to the reaction mixture that was stirred for 0.5 h and filtrated to remove the light yellow solid. The organic layer was collected, dried over $MgSO_4$, and evaporated. The crude product was purified through column chromatography (Hexane/CH_2Cl_2 = 50/1) to provide **11** as a white solid (0.39 g, 30%): m.p. 210-212 ℃. ^{1}H NMR (300 MHz, $CDCl_3$): δ 7.75-7.72 (m, 2H), 7.57-7.55 (m, 2H), 7.29-7.27 (m, 6H), 2.48 (s, 6H); ^{13}C NMR (75 MHz, CDCl3): δ 148.0, 139.5, 131.4, 129.9, 128.8, 127.2, 126.9, 126.4, 124.8, 121.6, 17.8. IT–TOF–MS (ESI): m/z $[M]^{2+}$ calcd. for $C_{22}H_{16}N_2O_4$ 186.0550, found 186.0547.

*3,3'-Bis(bromomethyl)-4,4'-dinitro-1,1'-binaphthalene (**2a**).* A solution of **11** (0.32 g, 0.86 mmol), NBS (0.32 g, 1.8 mmol), and AIBN (14.0 mg, 0.08 mmol) in benzene (20 mL) was heated to reflux with incandescent light and stirred for 24 h. Three additional portions of NBS (0.16 g, 0.9 mmol) and AIBN (7.0 mg, 0.04 mmol) were added at 24 h – intervals within 72 h. The mixture was allowed to cool to room temperature and evaporated. CH_2Cl_2 (50 mL) was added and the organic layer was washed with water, brine, dried with anhydrous Na_2SO_4, and concentrated under reduced pressure, then purified through column chromatography (Hexane/CH_2Cl_2 = 20/1) to give **2a** (87 mg, 19%) as white solid: m.p. 166-168 ℃. ^{1}H NMR (300 MHz, $CDCl_3$): δ 8.50 (d, J = 8.4 Hz, 2H), 7.65-7.60 (m, 2H), 7.55 (s, 2H), 7.40-7.32 (m,4H),4.91 (s, 4H); ^{13}C NMR (75 MHz, $CDCl_3$): δ 137.4, 134.6, 133.4, 132.5, 129.4, 128.1, 128.0, 127.6, 126.7, 125.3, 34.5. IT–TOF–MS (ESI): m/z $[M]^+$ calcd. for $C_{22}H_{14}Br_2N_2O_4$ 527.9315, found 527.9310.

*1,1'-(4,4'-Dinitro-[1,1'-binaphthalene]-3,3'-diyl)bis(N,N,N-trimethylmethanaminium) bromide (**3a**).* A 4.2 M trimethylamine solution in ethanol (2.4 mL, 10 mmol) was added to a mixture of **2a** (530.2 mg, 1 mmol) in EtOAc (10 mL). The reaction mixture was stirred at room temperature for 24 h and filtrated to give **3a** (596.5 mg, 92%) as a white solid: m.p. 236-238 ℃; ^{1}H NMR (500 MHz, CD_3OD): δ 8.64 (d, J =

8.7 Hz, 2H), 7.98 (s, 2H), 7.79 (t, J = 8.1 Hz, 2H), 7.57 (t, J = 6.9 Hz, 2H), 7.45 (d, J = 8.4 Hz, 2H), 5.19 (q, J = 15.6 Hz, 4H), 3.38 (s, 18H); ^{13}C NMR (125 MHz, CD_3OD): δ 137.3, 134.2, 132.6, 131.9, 129.5, 128.9, 128.8, 126.6, 125.9, 68.6, 52.9. IT–TOF–MS (ESI): m/z $[M]^+$ calcd. for $C_{28}H_{32}Br_2N_4O_4$ 646.0785, found 646.0781.

*4,4'-Dibromo-3,3'-bis(bromomethyl)-1,1'-binaphthalene (**2b**).* A solution of **5** (5.3 g, 12.0 mmol), NBS (4.27 g, 24.0 mmol), and AIBN (0.20 g, 1.20 mmol) in benzene (50 mL) was heated to reflux and stirred for 6 h. The reaction mixture was allowed to cool to room temperature and evaporated. CH_2Cl_2 (50 mL) was added and the organic layer was washed with water (50 mL), brine (50 mL), dried over anhydrous sodium sulfate, and concentrated under reduced pressure, then purified through column chromatography (Hexane/CH_2Cl_2 = 50/1) to give **2b** (3.80 g, 53%) as a white solid: m.p. 154-156 ℃; ^{1}H NMR (300 MHz, $CDCl_3$): δ 8.49-8.45 (m, 2H), 7.66-7.61 (m, 2H), 7.56-7.54 (m, 2H), 7.38-7.35 (m, 4H), 4.90 (s, 4H); ^{13}C NMR (75 MHz, $CDCl_3$): δ 137.4, 134.6, 133.4, 132.5, 129.4, 128.1, 128.0, 127.6, 126.7, 125.3, 34.5. IT–TOF–MS (ESI): m/z $[M]^+$ calcd. for $C_{22}H_{14}Br_4$ 593.7823, found 593.7820.

*1,1'-(4,4'-Dibromo-[1,1'-binaphthalene]-3,3'-diyl)bis(N,N,N-trimethylMethanaminium) bromide (**3b**).* A 4.2 M trimethylamine solution in ethanol (2.4 mL, 10 mmol) was added to a mixture of **2b** (598 mg, 1.0 mmol) in EtOAc (10 mL). The reaction mixture was stirred at room temperature for 24 h and filtrated to give **3b** (680 mg, 93% yield) as a white solid: m.p. 246-248 ℃; ^{1}H NMR (300 MHz, CD_3OD): δ 8.58 (t, J = 7.8 Hz, 2H), 7.91 (s, 2H), 7.74 (d, J = 8.1 Hz, 2H), 7.52 (d, J = 6.9 Hz, 2H), 7.40 (t, J = 7.8 Hz, 2H), 5.18-5.09 (m, 4H), 3.34 (s, 18H); ^{13}C NMR (75 MHz, CD_3OD): δ 137.3, 134.2, 132.6, 131.9, 129.5, 128.9, 128.8, 128.6, 126.6, 125.9, 68.6, 52.9. IT–TOF–MS (ESI): m/z $[M\text{-}2Br]^{2+}$ calcd. for $C_{28}H_{32}Br_2N_2$ 277.0461, found 277.0459.

*3,3'-Bis(bromomethyl)-1,1'-binaphthalene (**2c**).* A solution of **10** (3.39 g, 12.0 mmol), NBS (4.27 g, 24.0 mmol), and AIBN (0.20 g, 1.20 mmol) in benzene (50 mL) was heated to reflux and stirred for 6 h. The mixture was allowed to cool to room temperature and evaporated. CH_2Cl_2 (50 mL) was added and the organic layer was washed with water (50 mL), brine (50 mL), dried over anhydrous sodium sulfate,

concentrated under reduced pressure, then purified through column chromatography (Hexane/CH_2Cl_2 = 20/1) to give **2c** (2.06 g, 39% yield) as a white solid: m.p. 160-162 ℃; ^{1}H NMR (300 MHz, $CDCl_3$): δ 7.87-7.84 (m, 4H), 7.46-7.41 (m, 4H), 7.27-7.25 (m, 4H), 4.64 (s, 4H); ^{13}C NMR (75 MHz, $CDCl_3$): δ 138.7, 134.7, 133.4, 132.4, 128.6, 128.3, 128.0, 126.8, 126.5, 126.3, 33.8; IT–TOF–MS (ESI): m/z $[M]^{2+}$ calcd. for $C_{22}H_{16}Br_2$ 218.9804, found 218.9804.

*1,1'-([1,1'-Binaphthalene]-3,3'-diyl)bis(N,N,N-trimethylmethanaminium) bromide (**3c**).* A 4.2 M trimethylamine solution in ethanol (2.4 mL, 10 mmol) was added to a mixture of **2c** (438 mg, 1.0 mmol) in EtOAc (10 mL). The reaction mixture was stirred at room temperature for 24 h and filtrated to give **3c** (513 mg, 92% yield) as a white solid: m.p. 147-150 ℃. ^{1}H NMR (300 MHz, DMSO): δ 8.33 (s, 2H), 8.18 (d, J = 8.1 Hz, 2H), 7.71 (s, 2H), 7.66 (t, J = 7.5 Hz, 2H), 7.49 (t, J = 6.9 Hz, 2H), 7.40 (d, J = 8.4 Hz, 2H), 4.85 (s, 4H), 3.18 (s, 18H); ^{13}C NMR (75 MHz, CD_3OD): δ 140.1, 135.1, 134.7, 134.6, 132.1, 130.2, 129.4, 128.4, 127.2, 126.4, 70.4, 53.5; IT–TOF–MS (ESI): m/z $[M\text{-}2Br]^{2+}$ calcd. for $C_{28}H_{34}N_2$ 199.1356, found 199.1351.

*3,3'-Dimethyl-4,4'-diphenyl-1,1'-binaphthalene (**12**).* K_2CO_3 (4.2 mL, 2 M in water) was added to a mixture of **5** (0.44 g, 1.00 mmol), $PhB(OH)_2$ (0.43 g, 3.50 mmol), and $Pd(PPh_3)_4$ (0.17 g, 0.15 mmol) in THF (15 mL) under nitrogen. The reaction mixture was heated to reflux and stirred under refluxing for 24 h. Water (15 mL) was added to quench the reaction. Then, the crude products were extracted with CH_2Cl_2 (3 x 15 mL). The organic layer was dried over anhydrous Na_2SO_4, concentrated under reduced pressure, then purified through column chromatography (Hexane/CH_2Cl_2 = 30/1) to give **12** (0.29 g, 66%) as a white solid: m.p. 243-246 ℃; ^{1}H NMR (300 MHz, $CDCl_3$): δ 7.46-7.16 (m, 20H) , 2.23 (s, 6H); ^{13}C NMR (75 MHz, $CDCl_3$): δ 139.9, 138.0, 137.8, 133.0, 132.6, 131.4, 130.6, 130.3, 130.3, 128.4, 127.1, 126.6, 126.4, 125.6, 124.8, 20.8; IT–TOF–MS(ESI): m/z $[M+H]^+$ calcd. for $C_{34}H_{27}$ 435.2107, found 435.2103.

*3,3'-Bis(bromomethyl)-4,4'-diphenyl-1,1'-binaphthalene (**2d**).* A solution of **12** (5.21 g, 12.0 mmol), NBS (4.27 g, 24.0 mmol), and AIBN (0.20 g, 1.20 mmol) in benzene (50 mL) was heated to reflux and

stirred for 6 h. The reaction mixture was allowed to cool to room temperature and evaporated. CH_2Cl_2 (50 mL) was added and the organic layer was washed with water (50 mL), brine (50 mL), dried over anhydrous sodium sulfate, and concentrated under reduced pressure, then purified through column chromatography (Hexane/CH_2Cl_2 = 20/1) to give **2d** (3.13 g, 44% yield) as a white solid: m.p. 287-289 ℃; ^{1}H NMR (300 MHz, $CDCl_3$): δ 7.71 (brs, 2H), 7.56 (brs, 12H), 7.50 (brs, 2H), 7.37 (brs, 4H), 4.50 (s, 4H); ^{13}C NMR (75 MHz, $CDCl_3$): δ 139.4, 138.3, 137.6, 133.0, 132.7, 132.4, 130.3, 130.1, 129.5, 128.5, 127.9, 127.4, 126.6, 126.5, 127.3, 32.8; IT–TOF–MS (ESI): m/z $[M+3H]^{3+}$ calcd. for $C_{34}H_{24}Br_2$ 197.6821, found 197.6825.

*1,1'-(4,4'-Diphenyl-[1,1'-binaphthalene]-3,3'-diyl)bis(N,N,N-trimethylmethanaminium) bromide (**3d**).* A 4.2 M trimethylamine solution in ethanol (2.4 mL, 10 mmol) was added to a mixture of **2d** (592 mg, 1 mmol) in EtOAc (10 mL). The reaction mixture was stirred at room temperature for 24 h and filtrated to give **3d** (661 mg, 93% yield) as a white solid: m.p. 258-260 ℃; ^{1}H NMR (300 MHz, CD_3OD): δ 8.03 (d, J = 6.0 Hz, 2H), 7.73-7.60 (m, 8H), 7.57-7.45 (brs, 10H), 4.85 (s, 4H), 3.05 (s, 18H); ^{13}C NMR (75 MHz, CD_3OD): δ 145.8, 139.4, 138.3 135.0, 134.5, 132.8, 132.6, 130.3, 129.9, 129.1, 129.0, 128.3, 127.6, 124.0, 124.0, 68.0, 54.2; IT–TOF–MS (ESI): m/z $[M-2Br]^{2+}$ calcd. for $C_{40}H_{42}N_2$ 275.1669, found 275.1663.

Methyl 1-methoxy-2-naphthoate (7). K_2CO_3 (49.2g, 355.8 mmol) and CH_3I (9.9 mL, 159.3 mmol) were added to a solution of **6** (10.0 g, 53.1 mmol) in acetone (150 mL). The reaction mixture was stirred at 55℃ overnight until the reaction was completed. The solvent was removed under vacuum and water (250 mL) was added to the residue. The crude products were extracted with EtOAc (3 × 50 mL) and the organic phase was dried over Na_2SO_4, concentrated, and purified by column chromatography (Hexane/ EtOAc = 20/1) over silica gel to yield **7** (9.8 g, 85%) as a white solid. ^{1}H NMR (300 MHz, $CDCl_3$): δ 8.32 (brs, 1H), 7.89-7.87 (M, 2H), 7.65-7.59 (m, 3H), 4.12 (s, 3H), 4.02 (s, 3H) (the NMR spectra were in agreement with those reported).[28]

*Dimethyl 4,4'-dimethoxy-[1,1'-binaphthalene]-3,3'-dicarboxylate (**8**).* Boron trifluoride diethyl etherate (20 mL) was added to a solution of **7** (17.30 g, 0.08 mol) and lead tetraacetate (19.52 g, 0.044 mol) in acetonitrile (100 mL). The reaction mixture was stirred overnight, then poured into water (300 mL). The crude products were extracted with dichloromethane (2 x 300 mL). The organic layer was dried over Na_2SO_4 and evaporated. The crude product was passed through a short column of basic alumina using hexane as eluent to remove the Pb and highly colored polymeric materials, then purified through column chromatography (2.5% EtOAc/Hexane) to provide **5** (7.27 g, 42% yield) as a white solid: m.p. 200-203 ℃; ^{1}H NMR (300 MHz, $CDCl_3$): δ 8.44 (brs, 2H), 7.92 (s, 1H), 7.71-7.68 (m, 2H), 7.62-7.57 (m, 2H), 7.46-7.34 (m, 2H), 7.18 (d, J = 8.7 Hz, 1H), 4.20 (s, 6H), 3.99 (s, 6H); ^{13}C NMR (75 MHz, $CDCl_3$): δ 166.6, 166.4, 158.3, 158.2, 137.6, 136.1, 135.9, 133.6, 133.2, 130.5, 128.8, 128.7, 128.6, 128.6, 128.4, 126.7, 126.7, 126.6, 126.1, 123.9, 123.8, 122.1, 119.2, 118.7, 63.6, 52.3. IT–TOF–MS (ESI): m/z $[M+H]^+$ calcd. for $C_{26}H_{23}O_6$ 431.1489, found 431.1480.

*(4,4'-Dimethoxy-[1,1'-binaphthalene]-3,3'-diyl)dimethanol (**9**).* A solution of **8** (200.0 mg, 0.46 mmol) in THF was added $LiAlH_4$ (52.0 mg, 1.38 mmol). After stirring for 1 h, the reaction mixture was poured into water and extracted with EtOAc (3 × 50 mL). The organic phase was dried over Na_2SO_4, concentrated, and purified by column chromatography (Hexane/CH_2Cl_2 = 50/1) over silica gel to yield **9** as a white solid (155.0 mg, 90%): m.p. 137-139 ℃; ^{1}H NMR (300 MHz, CD_3OD): δ 8.24 (t, J = 8.4 Hz, 2H), 7.67-7.57 (m, 2H), 7.54-7.46 (m, 2H), 7.38 (d, J = 8.1 Hz, 0.5H), 7.29-7.25 (m, 3H), 7.11 (d, J = 8.7 Hz, 0.5H), 4.93 (s, 4H), 4.07 (s, 6H); ^{13}C NMR (75 MHz, CD_3OD): δ 153.1, 153.1, 138.5, 134.6, 134.4, 133.9, 133.8, 133.6, 129.1, 128.8, 128.4, 128.2, 128.0, 127.8, 126.4, 126.3, 125.7, 125.6, 125.2, 122.4, 122.0, 121.7, 61.9, 58.4; IT–TOF–MS (ESI): m/z $[M+Na]^+$ calcd. for $C_{24}H_{22}O_4Na$ 397.1416, found 397.1412.

*3,3'-Bis(bromomethyl)-4,4'-dimethoxy-1,1'-binaphthalene (**2e**).* PBr_3 (0.4 mL, 3.84 mmol) was added into a solution of **9** (720.0 mg, 1.92 mmol) in 30 mL of CH_2Cl_2. The reaction mixture was stirred at room temperature for 1 h, poured into water (50 mL), and extracted with CH_2Cl_2 (3 x 50 mL). The

organic phase was dried over Na_2SO_4, concentrated, and purified by column chromatography (Hexane/CH_2Cl_2 = 1/1) over silica gel to provide **2e** as a white solid (683.0 mg, 71%): m.p. 86-89 ℃; ^{1}H NMR (500 MHz, DMSO-*d*): δ 8.22(d, *J* = 8.5 Hz, 2H), 7.61 (t, *J* = 7.5 Hz, 2H), 7.56 (s, 2H), 7.42 (t, *J* = 8.0 Hz, 2H), 7.22 (d, *J* = 8.5 Hz, 2H), 4.96 (q, *J* = 7.0 Hz, 4H), 4.11 (s, 6H); ^{13}C NMR (75 MHz,): δ 134.5, 130.0, 129.8, 129.0, 127.9, 127.0, 126.4, 125.8, 123.3, 122.7, 62.7, 28.2; IT–TOF–MS (ESI): m/z [M^+] calcd. for $C_{24}H_{20}Br_2O_2$ 497.9825, found 497.9821.

*1,1'-(4,4'-Dimethoxy-[1,1'-binaphthalene]-3,3'-diyl)bis(N,N,N-trimethylmethanaminium) bromide (**3e**).* A 4.2 M trimethylamine solution in ethanol (2.4 mL, 10 mmol) was added to a mixture of **2e** (500 mg, 1.0 mmol) in EtOAc (10 mL). The reaction mixture was stirred at room temperature for 24 h and filtrated to give **3e** (575 mg, 93% yield) as a white solid: m.p. 273-275℃; ^{1}H NMR (300 MHz, CD_3OD): δ 8.38 (t, *J* = 8.7 Hz, 2H), 7.86-7.64 (m, 4H), 7.50 (t, *J* = 7.2 Hz, 2H), 7.43-7.26 (m, 2H), 4.76 (s, 4H), 4.14 (s, 6H), 3.27 (s, 18H). ^{13}C NMR (75 MHz, CD_3OD): δ 158.0, 157.8, 157.8, 137.8, 135.7, 135.6, 135.4, 134.8, 134.3, 131.6, 131.2, 130.0, 129.8, 128.1, 128.1, 127.9, 127.7, 127.6, 126.8, 126.7, 126.6, 126.4, 123.1, 122.8, 116.6, 116.3, 116.2, 64.0, 62.8, 52.3. IT–TOF–MS (ESI): m/z [M-2Br]$^{2+}$ calcd. for $C_{30}H_{38}N_2O_2$ 229.1461, found 229.1457.

General procedure for trapping assay.

Radical trapping: A reaction mixture of **2b** (200 mg, 0.33 mmol, 1.0 eq) or **3b** (200 mg, 0.28 mmol, 1.0 eq) and TEMPO (10.0 eq) in CH_3CN (2 mL) was irradiated with 350 nm UV light for around 3 days till all starting materials were consumed. The solvent was removed and the residue was purified by column chromatography (Hexane/EtOAc = 50/1) to afford the trapping adduct **18** as a white solid (103 mg, 42% yield for **2b**; 114 mg, 54% yield for 3**b**).

*1,1'-(((4,4'-Dibromo-[1,1'-binaphthalene]-3,3'-diyl)bis(methylene))bis(oxy))bis(2,2,6,6-tetramethylpiperidine) (**18**).* ^{1}H NMR (300 MHz, $CDCl_3$): δ 8.49 (s, 2H), 7.81 (s, 2H), 7.61 (s, 2H), 7.43 (s, 2H), 7.36 (s, 4H), 1.55 (s, 12H), 1.31 (s, 12H), 1.15 (s, 12H). ^{13}C NMR (75 MHz, $CDCl_3$): δ 137.5,

136.0, 133.1, 132.1, 128.2, 127.4, 127.3, 127.0, 126.5, 121.9, 78.8, 60.1, 39.8, 33.1, 33.0, 20.5, 17.1, 1.0. IT–TOF–MS (ESI): m/z $[M]^{2+}$ calcd. for $C_{40}H_{50}Br_2N_2O_2$ 374.1114, found 374.1110.

Carbocation trapping: Trimethylamine (3.0 mL, 22.00 mmol) was added to a solution of $MeONH_2 \cdot HCl$ (1.67 g, 20.00 mmol) in DMF (2 mL) and stirred at room temperature for 30 min. Then, **22** (150.00 mg, 0.50 mmol) in DMF (2 mL) was added. The resulting mixture was stirred for 20 min and irradiated with 350 nm light until the starting material was consumed (around 24 hours**)**. The reaction mixture was quenched by water (3 mL) and extracted with ethyl acetate (3 × 3 mL). The combined organic phase was washed with brine (3 mL) and dried over anhydrous Na_2SO_4. After removal of the solvent, the residue was purified by column chromatography (Hexane/EtOAc = 20/1) to provide the corresponding trapping adduct **23** (49 mg, 37% yield).

*N-((1-Bromonaphthalen-2-yl)methyl)-O-methylhydroxylamine (**23**).* ^{1}H NMR (300 MHz, $CDCl_3$): δ 8.36 (d, J = 8.4 Hz, 1H), 7.83 (t, J = 8.4 Hz, 2H), 7.64-7.51 (m, 3H), 6.06 (s, 1H), 4.44 (s, 2H), 3.60 (s, 3H). ^{13}C NMR (75 MHz, $CDCl_3$): δ 135.1, 134.0, 132.4, 128.2, 128.1, 127.6, 127.4, 127.3, 126.5, 124.3, 61.7, 56.8. IT–TOF–MS (ESI): m/z $[M^+]$ calcd. for $C_{12}H_{12}BrNO$ 265.0097, found 265.0095.

ICL formation with duplex DNA 13.

The ^{32}P-labelled oligonucleotide (0.5 μM) was annealed with 1.5 equiv of the complementary strand by heating to 90 ℃ for 5 min in potassium phosphate buffer (pH 7, 10 mM), followed by naturally cooling to room temperature. The ^{32}P-labeled ODN duplex (2 μL, 0.5 μM) was mixed with 1 M NaCl (2 μL), 100 mM potassium phosphate (2 μL, pH 8), and compounds **1-3** (concentration range: 10 μM to 2 mM in 6 μL CH_3CN). Then, the appropriate amount of autoclaved distilled water was added to give a final volume of 20 μL. The reaction was irradiated at 350 nm till the reaction was completed, then quenched with an equal volume of 90% formamide loading buffer and subjected to 20% denaturing PAGE analysis.

Trapping assay of oligonucleotides.

The ^{32}P-labeled oligonucleotide duplex (2 μL, 0.5 μM) was mixed with 1 M NaCl (2 μL), 100 mM potassium phosphate (2 μL, pH 8). The stock solution of $MeONH_2 \cdot HCl$ (2 M) was titrated with 5 M

NaOH to adjust the pH to ~ 7.0, which was diluted to the desired concentration (100/3 μM to 2000/3 mM). Then, 3 μL was added to the reaction mixture as appropriate for the desired concentration (final $MeONH_2$ concentration: 50 μM to 100 mM). Similarly, 3 μL of TEMPO in CH_3CN (100/3 μM to 2000/3 mM) was added to the reaction mixture as appropriate for the desired concentration (final TEMPO concentration: 50 μM to 100 mM). Compounds **1-3** (0.5 mM in 6 μL CH_3CN or water) and the appropriate amount of autoclaved distilled water to give a final volume of 20 μL (CH_3CN/H_2O: a final ratio of 3:7). The reaction mixture was irradiated at 350 nm till the reaction was completed, quenched with an equal volume of 90% formamide loading buffer, then subjected to 20% denaturing PAGE analysis.

Stability study of DNA ICL product formed with 13.

The ^{32}P-labeled oligonucleotide duplex **13** (30 μL, 0.5 μM) was mixed with 1 M NaCl (6 μL), 100 mM potassium phosphate (6 μL, pH 8) and 20/3 mM **2a-e** (18 μL CH_3CN), or **3a-e** (18 μL in H_2O). The solution was irradiated with 350 nm light for 4 h. After the cross-link reaction, the reaction mixtures (0.25 μM DNA duplex, 60 μL) were co-precipitated with calf thymus DNA (2.5 mg/mL, 20 μL) and NaOAc (3 M, 10 μL) in the presence of EtOH (90 μL) at -80 ℃ for 30 min, followed by centrifuging for 5 min at 15000 rmp. The supernatant was removed, and the pellet was co-precipitated with NaOAc (3 M, 5 μL) and H_2O (30 μL) in the presence of EtOH (120 μL) at -80 ℃ for 30 min again, followed by centrifuging for 5 min at 15000 rmp. The supernatant was removed and the pellet was lyophilized for 30 min in a Centrivap Concentrator of LABCONCO at 37 ℃. The dried DNA fragments were dissolved in H_2O (45 μL) and divided into three portions. One portion (20 μL) was incubated with piperidine (10 M, 10 μL) and H_2O (70 μL) at 90 ℃ for 30 min, and the second portion (20 μL) was incubated with NaCl (1.0 M, 10 μL) and 10 mM potassium phosphate buffer (pH 7, 10 μL) under the same condition, and the third portion (5 μL) was used as a control sample. The samples were subjected to 20% denaturing PAGE analysis.

Stability study of ICL products formed with 13 and **3b.** The ^{32}P-labeled oligonucleotide duplex **13** (30 μL, 0.5 μM) was mixed with 1 M NaCl (6 μL), 100 mM potassium phosphate (6 μL, pH 8), and

20/3 mM **3b** in H_2O (18 μL). The solution was irradiated with 350 nm light for10 h. After the cross-linking reaction was done, the DNA ICL products and monoalkylated ODNs were purified by gel electrophoresis. The isolated DNA fragments were dissolved in H_2O (60 μL) and divided into three portions. One portion (20 μL) was incubated with 1.0 M piperidine (10 μL) at 90 ^oC for 30 min, and the second portion (20 μL) was incubated with 0.1 M NaCl and 10 mM potassium phosphate buffer (pH 7, 10 μL) under the same condition, and the third portion (20 μL) was used as a control sample. The samples were subjected to electrophoresis on a 20% denaturing polyacrylamide gel.

Hydroxyl radical reaction (Fe·EDTA reaction). The cross-linked DNAs formed with duplex **27** and **3b** were purified by 20% denaturing PAGE. The band containing cross-linked product was cut, crushed, and eluted with 200 mM NaCl, 20 mM EDTA (2.0 mL). The crude product was further purified by C18 column eluting with H_2O (3 × 1.0 mL) followed by MeOH:H_2O (3:2, 1.0 mL). Fe(II)·EDTA cleavage reactions of ^{32}P-labelled oligonucleotide (0.1μM) were performed in a buffer containing 50 μM $(NH_4)_2Fe(SO_4)_2$, 100 μM EDTA, 5 mM sodium ascorbate, 0.5 M NaCl, 50 mM sodium phosphate (pH 7.5) and 5 mM H_2O_2 for 2 min at room temperature (total substrate volume 20 μL), then quenched with 100 mM thiourea (10 μL). Samples were lyophilized, dissolved in 20 μL H_2O: 90% formamide loading buffer (1:1) and subjected to 20% denaturing PAGE analysis.

Synthesis of 2b-dC, 2b-dA, and 2b-dG adducts.

Compound **2b** (239 mg, 0.4 mmol, 2 eq.) was added to a solution of dA, dT, dG, or dC (0.2 mmol, 1eq.) in DMF (1.0 mL), which was irradiated with 350 nm light at room temperature for 3 days. After removal of the solvent under reduced pressure, the crude products were isolated upon purification by column chromatography.

4-(((4,4'-Dibromo-3'-(hydroxymethyl)-[1,1'-binaphthalene]-3-yl)methyl)amino)-1-((2R,4S,5R)-4-hydroxy-5-(hydroxymethyl)tetrahydrofuran-2-yl)pyrimidin-2(1H)-one ***(24)***. 112 mg, 41% yield. ^{1}H NMR (500 MHz, DMSO-*d*): 8.41 (d, *J* = 8.5 Hz, 2H), 7.74 (t, *J* = 8.5 Hz, 2H), 7.68 (d, *J* = 13.5 Hz,

1H), 7.51-7.44 (m, 2H), 7.32-7.19 (m, 3H), 7.01 (s, 1H), 6.12 (s, 1H), 5.83 (t, *J* = 6.5 Hz, 1H), 5.47 (t, *J* = 9.5 Hz, 1H), 5.40 (d, *J* = 16.5 Hz, 1H), 5.20 (s, 1H), 5.13 (s, 1H), 5.04 (s, 1H), 4.91 (s, 1H), 4.17 (s, 1H), 3.72 (s, 1H), 3.50 (s, 2H), 2.10 (s, 1H), 2.02-1.95 (m, 2H). IT–TOF–MS (ESI): m/z [M^+] calcd. for $C_{31}H_{27}Br_2N_3O_5$ 679.0312, found 679.0310.

*6-Amino-7-((4,4'-dibromo-3'-(hydroxymethyl)-[1,1'-binaphthalene]-3-yl)methyl)-9-((2S,4R,5S)-4-hydroxy-5-(hydroxymethyl)tetrahydrofuran-2-yl)-9H-purin-7-ium (**25a**)*. 138 mg, 49% yield. ^{1}H NMR (500 MHz, DMSO-*d*): 8.41 (t, *J* = 7.0 Hz, 2H), 8.34 (t, *J* = 8.5 Hz, 1H), 8.24 (s, 1H), 7.74-7.69 (m, 2H), 767 (s, 1H), 7.47-7.42 (m, 2H), 7.24 (d, *J* = 6.5 Hz, 2H), 7.14 (s, 1H), 6.21 (t, *J* = 6.5 Hz, 1H), 5.63 (s, 2H), 5.33 (s, 1H), 5.00 (s, 1H), 4.37 (s, 1H), 3.85 (s, 1H), 3.58-3.50 (m, 2H), 3.19 (s, 1H), 2.60-2.51 (m, 1H), 2.27-2.24 (m, 1H). IT–TOF–MS (ESI): m/z [M^+] calcd. for $C_{32}H_{28}Br_2N_5O_4$ 704.0503, found 704.0507.

ASSOCIATED CONTENT

Supporting Information

UV absorption spectra, NMR and HRMS spectra, representative gels for DNA cross-link assay, effects of TEMPO and methoxyamine on DNA ICL formation, and piperidine treatment of the cross-linked products. This material is available free of charge via the Internet at http://

AUTHOR INFORMATION

Corresponding Author

Fax: (+01)414-2295530, Email: pengx@uwm.edu.

Notes

The authors declare no competing financial interests.

ACKNOWLEDGMENT

This work was supported by the National Cancer Institute - 1R15CA152914-01, Great Milwaukee Foundation (Shaw Scientist Award), UWM Research Foundation Catalyst Grant, and the University of Wisconsin Milwaukee Research Growth Initiative.

REFERENCES

[1] Fan, H.; Peng, X. (2016) Novel DNA Cross-Linking Reagents, *in Advances in Molecular Toxicology, 10*, pp. 235-292.
[2] Percivalle, C., Doria, F., and Freccero, M. (2014) Quinone Methides as DNA Alkylating Agents: An Overview on Efficient Activation Protocols for Enhanced Target Selectivity, *Curr Org Chem 18*, 19-43.
[3] Deans, A. J., and West, S. C. (2011) DNA interstrand crosslink repair and cancer, *Nat Rev Cancer 11*, 467-480.
[4] Ashwood-Smith, M. J., Poulton, G. A., Barker, M., and Mildenberger, M. (1980) 5-Methoxypsoralen, an ingredient in several suntan preparations, has lethal, mutagenic and clastogenic properties, *Nature 285*, 407-409.
[5] Peng, X., Ghosh, A. K., Van Houten, B., and Greenberg, M. M. (2010) Nucleotide excision repair of a DNA interstrand cross-link produces single- and double-strand breaks, *Biochemistry 49*, 11-19.
[6] Majumdar, A., Muniandy, P. A., Liu, J., Liu, J. I., Liu, S. T., Cuenoud, B., and Seidman, M. M. (2008) Targeted gene knock in and sequence modulation mediated by a psoralen-linked triplex-forming oligonucleotide, *J Biol Chem 283*, 11244-11252.
[7] Cahova, H., and Jaschke, A. (2013) Nucleoside-Based Diarylethene Photoswitches and Their Facile Incorporation into Photoswitchable DNA, *Angew Chem Int Edit 52*, 3186-3190.
[8] Haque, M. M., Sun, H., Liu, S., Wang, Y., and Peng, X. (2014) Photoswitchable formation of a DNA interstrand cross-link by a coumarin-modified nucleotide, *Angew. Chem. Int. Ed. Engl. 53*, 7001-7005.
[9] Wang, P., Liu, R., Wu, X., Ma, H., Cao, X., Zhou, P., Zhang, J., Weng, X., Zhang, X. L., Qi, J., Zhou, X., and Weng, L. (2003) A potent, water-soluble and photoinducible DNA cross-linking agent, *J Am Chem Soc 125*, 1116-1117.
[10] Weng, X., Ren, L., Weng, L., Huang, J., Zhu, S., Zhou, X., and Weng, L. (2007) Synthesis and biological studies of inducible DNA cross-linking agents, *Angew. Chem. Int. Ed. Engl. 46*, 8020-8023.
[11] Di Antonio, M., Doria, F., Richter, S. N., Bertipaglia, C., Mella, M., Sissi, C., Palumbo, M., and Freccero, M. (2009) Quinone methides tethered to naphthalene diimides as selective G-quadruplex alkylating agents, *J Am Chem Soc 131*, 13132-13141.
[12] Richter, S. N., Maggi, S., Mels, S. C., Palumbo, M., and Freccero, M. (2004) Binol quinone methides as bisalkylating and DNA cross-linking agents, *J Am Chem Soc 126*, 13973-13979.
[13] Verga, D., Nadai, M., Doria, F., Percivalle, C., Di Antonio, M., Palumbo, M., Richter, S. N., and Freccero, M. (2010) Photogeneration and reactivity of naphthoquinone methides as purine selective DNA alkylating agents, *J Am Chem Soc 132*, 14625-14637.
[14] Lin, G., and Li, L. (2013) Oxidation and reduction of the 5-(2'-deoxyuridinyl)methyl radical, *Angew. Chem. Int. Ed. Engl. 52*, 5594-5598.
[15] Weng, L., Horvat, S. M., Schiesser, C. H., and Greenberg, M. M. (2013) Deconvoluting the reactivity of two intermediates formed from modified pyrimidines, *Org Lett 15*, 3618-3621.
[16] Han, Y., Chen, W., Kuang, Y., Sun, H., Wang, Z., and Peng, X. (2015) UV-Induced DNA Interstrand Cross-Linking and Direct Strand Breaks from a New Type of Binitroimidazole Analogue, *Chem. Res. Toxicol. 28*, 919-926.
[17] Wang, Y., Liu, S., Lin, Z., Fan, Y., Wang, Y., and Peng, X. (2016) Photochemical Generation of Benzyl Cations That Selectively Cross-Link Guanine and Cytosine in DNA, *Org Lett 18*, 2544-2547.
[18] Wang, Y. B., Lin, Z. C., Fan, H. L., and Peng, X. H. (2016) Photoinduced DNA Interstrand Cross-Link Formation by Naphthalene Boronates via a Carbocation, *Chem-Eur J 22*, 10382-10386.
[19] Doria, F., Richter, S. N., Nadai, M., Colloredo-Mels, S., Mella, M., Palumbo, M., and Freccero, M. (2007) BINOL-amino acid conjugates as triggerable carriers of DNA-targeted potent photocytotoxic agents, *J Med Chem 50*, 6570-6579.
[20] Chen, W., Han, Y., and Peng, X. (2014) Aromatic nitrogen mustard-based prodrugs: activity, selectivity, and the mechanism of DNA cross-linking, *Chem-Eur J 20*, 7410-7418.
[21] Kuang, Y., Balakrishnan, K., Gandhi, V., and Peng, X. (2011) Hydrogen peroxide inducible DNA cross-linking agents: targeted anticancer prodrugs, *J Am Chem Soc 133*, 19278-19281.
[22] Cao, S., Wang, Y., and Peng, X. (2012) ROS-inducible DNA cross-linking agent as a new anticancer prodrug building block, *Chem-Eur J 18*, 3850-3854.
[23] Maxam, A. M., and Gilbert, W. (1977) A new method for sequencing DNA, *Proc Natl Acad Sci U S A 74*, 560-564.
[24] Maxam, A. M., and Gilbert, W. (1980) Sequencing end-labeled DNA with base-specific chemical cleavages, *Methods Enzymol 65*, 499-560.
[25] Millard, J. T., Weidner, M. F., Kirchner, J. J., Ribeiro, S., and Hopkins, P. B. (1991) Sequence preferences of DNA interstrand crosslinking agents: quantitation of interstrand crosslink locations in DNA duplex fragments containing multiple crosslinkable sites, *Nucleic Acids Res 19*, 1885-1891.
[26] Maniatis, T. F., E. F.; Sambrook, J. Molecular Cloning: A Laboratory Manual (1982) *Cold Spring Harbor Laboratory, Cold Spring Harbor, NY.*
[27] A. McKillop, A. G. T., D. W. Young, E. C. Taylor,. (1980) *J. Am. Chem. Soc. 102*, 6504-6512.
[28] Brockway, A. J., Gonzalez-Lopez, M., Fettinger, J. C., and Shaw, J. T. (2011) Direct displacement of alkoxy groups of vinylogous esters by Grignard reagents, *J Org Chem 76*, 3515-3518.